AIMS Mathematics, 10(3): 7099–7126.
DOI: 10.3934/math.2025324
Received: 03 February 2025
Revised: 14 March 2025
Accepted: 21 March 2025
Published: 27 March 2025

https://www.aimspress.com/journal/Math

Research article

Novel Laplace-integrated least square methods for solving the fractional nonlinear damped Burgers' equation

M. Mossa Al-Sawalha[1], Khalil Hadi Hakami[2,*], Mohammad Alqudah[3], Qasem M. Tawhari[2] and Hussain Gissy[2]

[1] Department of Mathematics, College of Science, University of Ha'il, Ha'il 2440, Saudi Arabia
[2] Department of Mathematics, Faculty of Science, Jazan University, P.O. Box 2097, Jazan 45142, Kingdom of Saudi Arabia
[3] Department of Basic Sciences, School of Electrical Engineering & Information Technology, German Jordanian University, Amman 11180, Jordan

* **Correspondence:** Email: khakami@jazanu.edu.sa.

Abstract: In this paper, we investigate the fractional damped Burgers' equation using two efficient analytical approaches: the Laplace least squares residual power series method and the Laplace least squares variational iteration method. These techniques integrate the Laplace transform with the least squares residual power series and least squares variational iteration methods, providing highly accurate solutions for nonlinear fractional differential equations. The fractional derivatives are considered in the sense of the Caputo operator, allowing for a more realistic description of physical phenomena with memory effects. Comparative studies with exact and numerical solutions demonstrate the reliability and accuracy of the results. The proposed methodologies provide a powerful framework for solving nonlinear fractional models in fluid dynamics, shock wave theory, and applied sciences.

Keywords: fractional damped Burgers' equation; Laplace least squares residual power series method; Laplace least squares variational iteration method; Caputo fractional operators
Mathematics Subject Classification: 34A08, 35A15, 35A23

1. Introduction

Factional-order mathematical models and fractional calculus (FC) have several applications in applied sciences, engineering, plasma physics, and fluid mechanics due to their capacity to accurately and comprehensively portray a variety of issues and applications. A wide range of studies have applied these models, namely for modelling biological events and diseases [1, 2], modelling diffusive type circuits [3], conducting a thorough survey on fractional-order derivative-based techniques in

computer vision [4], and researching sensors, analogs, and digital filters [5]. Several early recommendations were given for the basic structure of FC and viewpoints on generalized calculus [6–10]. Numerous areas have employed FC due to its interesting and realistic implications related to temporal and hereditary aspects [11–16]. To reveal the physical essence of complex problems, fractional differential equations must be solved. This study adopts the Caputo fractional derivative because it provides beneficial applications to model physical and engineering problems. The Caputo derivative provides a solution for physical applications by handling traditional initial conditions along with fractional-order derivatives while differentiating from the requirements of the Riemann-Liouville derivative. The Caputo derivative offers a generalized mathematical approach using traditional differential equations, surpassing both Jumarie's and He's fractional derivatives, which are primarily employed in modified frameworks. When problems demand both initial conditions and solutions in continuous domains, the Caputo derivative proves to be a superior choice than Yang's local fractional derivative. The Caputo derivative provides this research with both traditional model alignment and accurate fractional system memory representation.

Due to their superior capabilities as shown in references [17–20], fractional partial differential equations (PDEs) may more successfully solve complex engineering and physical difficulties than usual integer-order PDEs. Furthermore, they have the capacity to simulate the intricate systems connected to the genetic or memory characteristics [21, 22], and their management of non-local interactions and long-term temporal dependency is a crucial advantage over conventional differential equations.

Since partial derivatives, which are calculated using different integral and derivative definitions in fractional calculus, allow us to analyze problems in greater depth, the numerical solutions of fractional PDEs (FPDEs) have started to be studied. The homotopy perturbation method for the fractional Lotka-Volterra equations and fractional Kdv-Burgers' equation [23, 24], the variational iteration approach for fractional Burgers' equation [25, 26], the homotopy analysis approach for fractional Chan-Allen equations and damped Burgers' equation [27], and the Adomian method for fractional wave and diffusion equations [28] have all been expanded upon. Many definitions of fractional derivatives and integrals have been established by authors who deal with fractional analysis in an effort to improve comprehension of the dynamics of real-world situations and address computational flaws. To further explain the dynamics of the issues, definitions of non-local and local fractional derivatives and integrals have been proposed in various works [29].

Consider the damped Burgers' equation of time-fractional order:

$$D_{\gamma}^{\mu}\zeta(\delta,\gamma)+\frac{\partial^2\zeta(\delta,\gamma)}{\partial\delta^2}+\zeta(\delta,\gamma)\frac{\partial\zeta(\delta,\gamma)}{\partial\delta}+\frac{1}{5}\zeta(\delta,\gamma)=0,\ \gamma>0,\ 0<\mu\leq 1. \tag{1.1}$$

The Eq (1.1) fractional form will be examined in the present study using the Caputo derivative. The damped Burgers' equation appears in the literature as an example of an equation for describing diffuse waves that are susceptible to diffusion in fluid mechanics. Furthermore, the numerical solutions of the nonlinear acoustics problem, which also occur as a model equation in gas dynamics, have been examined in [30, 31]. The approximate solution of the damped Burgers equation has been obtained by Malfliet using the tanh method as a perturbation approach [32]. Yilmaz and Karasozen solved optimum control issues for the unsteady Burgers equation using COMSOL Multiphysics [33].

Consider the fractional-order Rosenau-Hyman equation:

$$D_{\gamma}^{\mu}\zeta(\delta,\gamma)-\zeta(\delta,\gamma)\frac{\partial\zeta(\delta,\gamma)}{\partial\delta}-\zeta(\delta,\gamma)\frac{\partial^{3}\zeta(\delta,\gamma)}{\partial\delta^{3}}-3\frac{\partial\zeta(\delta,\gamma)}{\partial\delta}\frac{\partial^{2}\zeta(\delta,\gamma)}{\partial\delta^{2}}=0,\ \gamma>0,\ 0<\mu\leq 1. \tag{1.2}$$

The authors of the 1993 compactons experiment, Philip Rosenau and James M. Hyman, are honoured by this equation. The Rosenau-Hyman equation is a simple model for studying nonlinear dispersion in pattern formation in liquid droplets. It may also be used to illustrate a variety of physics and engineering problems [34]. In mathematical physics and applied sciences, the compactons explorations of the Rosenau-Hyman equation are particularly beneficial [35–38]. Through these applications, we are urged to solve this equation and learn more about their characteristics. There are several ways to solve the fractional Rosenau-Hyman problem, including the reduced differential transform approach [39], the homotopy perturbation method [40], the residual power series method and perturbation-iteration algorithm [41], the Genocchi wavelets method [42], and the Laplace homotopy analysis method [43].

In the present work, we analyze the fractional damped Burgers' equation and the Rosenau-Hyman equation using two novel methods: the Laplace least squares residual power series method (LLSRPSM) and the Laplace least squares variational iteration method (LLSVIM). The least square technique combined with these two methods [44–51] make them reliable and efficient for the solution of the fractional-order partial differential equation. These methods provide approximations easily that are closer to the exact solution. The solution obtained via these methods, along with the figures and tables, are compared and contrasted in the paper to show the reliability of these methods. This work also provides a framework for the solution of various types of nonlinear and linear PDEs.

2. Preliminaries

This section provides a systematic description of the Caputo fractional derivative (CFD) and fractional partial Wronskian (FPW).

Definition 2.1. *For the fractional-order $\mu \geq 0$, the fractional Riemann-Liouville (RL) integral according to [17, 52, 53] is given as*

$$\mathcal{J}^{\mu}\zeta(\gamma)=\begin{cases}\frac{1}{\Gamma(\mu)}\int_{0}^{\gamma}\frac{\zeta(s)}{(\gamma-s)^{1-\mu}}ds=\frac{1}{\Gamma(\mu)}\gamma^{\mu-1}, & \mu>0,\gamma>0,\\ \zeta(\gamma), & \mu=0,\end{cases}$$

where the convolution product of $\gamma^{\mu-1}$ and $\zeta(\gamma)$ is denoted by $\gamma^{\mu-1}\zeta(\gamma)$.

The subsequent characteristics are related to the fractional RL integral.

(1) $\mathcal{J}^{\mu}\gamma^{\nu}=\frac{\Gamma(\nu+1)}{\Gamma(\nu+1+\mu)}\gamma^{\nu+\mu},\ \nu>-1,$
(2) $\mathcal{J}^{\mu}(\lambda\zeta(\gamma)+\theta\mathcal{G}(\gamma))=\lambda\mathcal{J}^{\mu}\zeta(\gamma)+\theta\mathcal{J}^{\mu}\mathcal{G}(\gamma),$

where the real constants are λ and θ.

Definition 2.2. *For the fractional-order μ, the CFD according to [54, 55] is given as*

$$D^{\mu}\zeta(\gamma)=\frac{1}{\Gamma(1-\mu)}\int_{0}^{\gamma}\frac{\zeta^{\mu}(s)}{(\gamma-s)^{\mu+1-\mu}}ds,\ \mu-1<\mu\leq\mu,n\in N.$$

The CFD has the following properties:

(1) $D^{\mu}\mathcal{J}^{\mu}\zeta(\gamma) = \zeta(\gamma)$,
(2) $\mathcal{J}^{\mu}D^{\mu}\zeta(\gamma) = \zeta(\gamma) - \sum_{i=0}^{n-1} \mathcal{Y}^{i}(0)(\frac{\gamma^{i}}{i!})$,
(3) $D^{\mu}\gamma^{\nu} \begin{cases} \frac{\Gamma(\nu+1)}{\Gamma(\nu+1-\mu)}\gamma^{\nu-\mu}, & \nu \geq \mu, \\ 0, & \nu < \mu, \end{cases}$
(4) $D^{\mu}c = 0$,
(5) $D^{\mu}(\lambda\zeta(\gamma) + \theta\mathcal{G}(\gamma)) = \lambda D^{\mu}\zeta(\gamma) + \theta D^{\mu}\mathcal{G}(\gamma)$.

Definition 2.3. *[56] Consider n functions $\Psi_1, \Psi_2, \Psi_3 \cdots, \Psi_n$ of variables δ and γ, which are defined on domain I; then, FPW of $\Psi_1, \Psi_2, \Psi_3 \cdots, \Psi_n$ is*

$$\omega^{\mu}[\Psi_1, \Psi_2, \Psi_3 \cdots, \Psi_n] = \begin{vmatrix} \Psi_1 & \Psi_2 & \Psi_3 & \cdots & \Psi_n \\ D^{\mu}\Psi_1 & D^{\mu}\Psi_2 & D^{\mu}\Psi_3 & \cdots & D^{\mu}\Psi_n \\ D^{2\mu}\Psi_1 & D^{2\mu}\Psi_2 & D^{2\mu}\Psi_3 & \cdots & D^{2\mu}\Psi_n \\ \vdots & \vdots & \vdots & \vdots & \vdots \\ D^{(n-1)\mu}\Psi_1 & D^{(n-1)\mu}\Psi_2 & D^{(n-1)\mu}\Psi_3 & \cdots & D^{(n-1)\mu}\Psi_n \end{vmatrix}$$

where $D^{\mu}\Psi_k = (\frac{\partial}{\partial\delta} + \frac{\partial^{\mu}}{\partial\gamma^{\mu}})\Psi_k$ and $D^{n\mu} = D^{\mu}D^{\mu}D^{\mu}\cdots D^{\mu}(n - times)$ and $k = 1, 2, 3, \cdots n$.

Definition 2.4. *[56] Consider the FPW of the n functions $\Psi_1(\delta,\gamma), \Psi_2(\delta,\gamma), \Psi_3(\delta,\gamma), \cdots, \Psi_n(\delta,\gamma)$ at least one point of the domain $I = [a,b] \times [a,b]$ is not zero, then the functions $\Psi_1(\delta,\gamma), \Psi_2(\delta,\gamma), \Psi_3(\delta,\gamma), \cdots, \Psi_n(\delta,\gamma)$ are linearly independent.*

Definition 2.5. *Consider the exponential-order piecewise continuous function $\zeta(\delta,\gamma)$ in $I \times [0,\infty)$. Then, the Laplace transform (LT) of $\zeta(\delta,\gamma)$ according to [57] is given as:*

$$\zeta(\delta, s) = \mathcal{L}[\zeta(\delta,\gamma)] := \int_0^{\infty} e^{-s\gamma}\zeta(\delta,\gamma)d\gamma, \quad s > \varrho.$$

The Laplace inverse transform (LIT) for the function $\zeta(\delta, s)$ is described as follows:

$$\zeta(\delta,\gamma) = \mathcal{L}^{-1}[\zeta(\delta, s)] := \int_{c-i\infty}^{c+i\infty} e^{s\gamma}\zeta(\delta, s)ds, \quad c = \mathrm{Re}(s) > \varrho_0,$$

where the Laplace integral absolutely converges on the right half-plane, where ϱ_0 is located.

Lemma 2.1. *[57] Assume that the functions $\zeta(\delta,\gamma)$ and $\xi(\delta,\gamma)$ are continuous piecewise on the interval $I \times [0,\infty)$ and ϱ_1 and ϱ_2 are its exponential orders, respectively, where $\varrho_1 < \varrho_2$. Suppose that $\vartheta_1(\delta,\gamma) = \mathcal{L}[\zeta(\delta,\gamma)]$,$\vartheta_2(\delta,\gamma) = \mathcal{L}[\xi(\delta,\gamma)]$, and the arbitrary constants are a, b. Then, the subsequent characteristics are true.*

(1) $\mathcal{L}[a\zeta(\delta,\gamma) + b\xi(\delta,\gamma)] = a\vartheta_1(\delta, s) + b\vartheta_2(\delta, s),\ \delta \in I,\ s > \varrho_1$,
(2) $\mathcal{L}^{-1}[a\vartheta_1(\delta, s) + b\vartheta_2(\delta, s)] = a\zeta(\delta,\gamma) + b\xi(\delta,\gamma),\ \delta \in I,\ \gamma \geq 0$,
(3) $\mathcal{L}[e^{a\gamma}\zeta(\delta,\gamma)] = \vartheta_1(\delta, s-a),\ \delta \in I.\ s > a + \varrho_1$,
(4) $\lim_{s\to\infty} s\vartheta_1(\delta, s) = \zeta(\delta, 0),\ \delta \in I$.

Lemma 2.2. *[57] Let us assume the exponential-order and piecewise continuous function $\zeta(\delta,\gamma)$ on $I\times[0,\infty)$ and $\vartheta_1(\delta,\gamma)=\mathcal{L}[\zeta(\delta,\gamma)]$. Then, the subsequent characteristics are true:*

(1) $\mathcal{L}[\mathcal{J}\zeta(\delta,\gamma)=a^{\mu-1}\vartheta_1(\delta,s),\ \mu>0,$
(2) $\mathcal{L}D^{\mu}_{\gamma}[\zeta(\delta,\gamma)=a^{\mu}\vartheta_1(\delta,s)-\sum_{k=0}^{n-1}s^{\mu-k-1}D^{k\mu}_{\gamma}\zeta(\delta,0),\ n-1<\mu\leq n,$
(3) $\mathcal{L}D^{j\mu}_{\gamma}[\zeta(\delta,\gamma)=a^{j\mu}\vartheta_1(\delta,s)-\sum_{k=0}^{j-1}s^{(j-k)\mu-1}D^{k\mu}_{\gamma}\zeta(\delta,0),\ 0<\mu\leq 1,$ where $D^{j\mu}=D^{\mu}.D^{\mu}.D^{\mu}\cdots.D^{\mu}(j-$ *times*).

Theorem 2.3. *[57] Consider the exponential-order and piecewise continuous function $\zeta(\delta,\gamma)$ on $I\times[0,\infty)$. Let us consider that the function $\vartheta_1(\delta,s)=\mathcal{L}[\zeta(\delta,\gamma)]$ has the fractional expansion, which is given as:*

$$\vartheta_1(\delta,s)=\sum_{n=0}^{\infty}\frac{\hbar_r(\delta)}{s^{n\varphi+1}},\ \delta\in I,s>\varrho,\ 0<\mu\leq 1.$$

Then

$$\hbar_n(\delta)=D^{n\mu}_{\gamma}\zeta(\delta,0),$$

Remark 2.4. *In Theorem 2.3, the LIT for the function $\zeta(\delta,\gamma)=\mathcal{L}^{-1}\vartheta_1(\delta,s)$ is given as:*

$$\zeta(\delta,\gamma)=\sum_{n=0}^{\infty}D^{n\mu}_{\gamma}\zeta(\delta,0)\frac{\gamma^{n\mu}}{\Gamma(n\mu+1)},\ 0<\mu\leq 1,\ \gamma\geq 0.$$

Theorem 2.5. *[57] Consider the exponential-order and piecewise continuous function $\zeta(\delta,\gamma)$. Assume that in Theorem 2.3, the fractional expansion for the function $\vartheta_1(\delta,s)=\mathcal{L}[\zeta(\delta,\gamma)]$ is given below. If $\left|s\mathcal{L}[D^{(n+1)\mu}_{\gamma}]\zeta(\delta,\gamma)\right|\leq M(\delta)$ on $I\times(\delta,\gamma]$ where $0<\mu\leq 1$, then the remainder $R_n(\delta,s)$ of the fractional expansion in Theorem 2.3 validates the subsequent inequality:*

$$|R_n(\delta,s)|\leq\frac{M(\delta)}{s^{1+(n+1)\mu}},\ \delta\in I,\delta<s\leq\tau.$$

Theorem 2.6. *If $a\in(0,1)$, $\|\zeta_{k+1}(\delta,\gamma)\|\leq a\|\zeta_k(\delta,\gamma)\|$ gives $\forall\ k\in N$ and $0<\gamma<T<1$, then the series of numerical solutions converges to the exact solution [58]:*

Proof. Let us assume that $\forall\ 0<\gamma<T<1$,

$$\begin{aligned}\|\zeta(\delta,\gamma)-\zeta_k(\delta,\gamma)\|&=\|\sum_{m=k+1}^{\infty}\zeta_m(\delta,\gamma)\|\leq\sum_{m=k+1}^{\infty}\|\zeta_m(\delta,\gamma)\|\\&\leq\|(\eta)\|\|\sum_{m=k+1}^{\infty}C^m\|=\frac{\mu^{k+1}}{1-\mu}\|(\eta)\|\to 0\ as\ k\to\infty.\end{aligned}$$

□

3. The general implementation of Laplace least squares residual power series method

The general process of the Laplace least squares residual power series approach is provided in this section. For time-fractional differential equations, a combination of the Laplace residual power series and the least squares approach is employed, which is based on the traditional Laplace residual power series method.

3.1. Laplace residual power series method (LRPSM)

Assume the fractional-order nonlinear PDE

$$\begin{aligned} D_{\gamma}^{\mu}\zeta(\delta,\gamma) &= N_{\delta}[\zeta(\delta,\gamma)] \\ \zeta(\delta,0) &= f(\delta). \end{aligned} \tag{3.1}$$

The nonlinear operator N_δ is dependent on δ and has a degree of r. The $\delta \in I$, $\gamma \geq 0$, and the Caputo derivative for $\mu \in (0, 1]$ is represented by D_{γ}^{μ}, and we will have to find $\zeta(\delta, \gamma)$.

A number of steps may be taken in order to create an approximate solution for Eq (3.1) using the LRPSM:

Step 1: Utilize the starting constraint from Eq (3.1) and take the LT on Eq (3.1).

$$\begin{aligned} \zeta(\delta,s) &= \frac{f(\delta)}{s} - \frac{1}{s^{\mu}}\mathcal{L}\left\{N_{\delta}[\zeta(\delta,\gamma)]\right\}, \\ \text{where } \zeta(\delta,s) &= \mathcal{L}[\zeta(\delta,\gamma)](s), s > \gamma. \end{aligned} \tag{3.2}$$

Step 2: The fractional expansion for finding the solution of Eq (3.2) is given below:

$$\zeta(\delta,s) = \frac{f(\delta)}{s} + \sum_{n=1}^{\infty}\frac{h_n(x)}{s^{n\mu+1}}, x \in I, s > \gamma \geq 0. \tag{3.3}$$

One may obtain the k-th Laplace series solution as given below:

$$\zeta_k(\delta,s) = \frac{f(\delta)}{s} + \sum_{n=1}^{k}\frac{h_n(x)}{s^{n\mu+1}}, \delta \in I, s > \gamma \geq 0. \tag{3.4}$$

Step 3: Equation 3.2 has a k-th Laplace fractional residual function (LFRF) as stated below:

$$\mathcal{L}\left(\mathrm{Res}_k(\delta,s)\right) = \zeta_k(\delta,s) - \frac{f(\delta)}{s} + \frac{1}{s^{\mu}}\mathcal{L}\left\{N_{\delta}[\zeta_k(\delta,\gamma)]\right\}, \tag{3.5}$$

Hence the Laplace residual function (LRF) of Eq (3.2) has this definition:

$$\lim_{k\to\infty}\mathcal{L}\left(\mathrm{Res}_k(\delta,s)\right) = \mathcal{L}\left(\mathrm{Res}(\delta,s)\right) = \zeta(\delta,s) - \frac{f(\delta)}{s} + \frac{1}{s^{\mu}}\mathcal{L}\left\{N_{\delta}[\zeta(\delta,\gamma)]\right\}. \tag{3.6}$$

Key characteristics of the LRF that are necessary to determine the approximate solution are listed below:

(1) $\lim_{k\to\infty}\mathcal{L}\left(\mathrm{Res}_k(\delta,s)\right) = \mathcal{L}\left(\mathrm{Res}(\delta,s)\right)$, for $\delta \in I, s > \gamma \geq 0$,
(2) $\mathcal{L}\left(\mathrm{Res}(\delta,s)\right) = 0$, for $\delta \in I, s > \gamma \geq 0$,
(3) $\lim_{s\to\infty} s^{k\mu+1}\mathcal{L}\left(\mathrm{Res}_k(\delta,s)\right) = 0$, for $\delta \in I, s > \gamma \geq 0$, and $k = 1, 2, 3, \ldots$

Step 4: In the k-th LFRF of Eq (3.5), substitute the k-th Laplace series solution (LSS) Eq (3.4).
Step 5: For $k = 1, 2, 3, \ldots$, the unknown coefficients $h_k(\delta)$ might be obtained by solving the system $\lim_{s\to\infty} s^{k\mu+1}\mathcal{L}\left(\mathrm{Res}_k(\delta,s)\right) = 0$. Subsequently, we calculate the acquired coefficients using Eq (3.4).
Step 6: For the main Eq (3.1), the approximate solution $\zeta_k(\delta, \gamma)$ may be obtained by applying the LIT to both sides of the derived LSS.

3.2. Laplace least square residual power series method (LLSRPSM)

This section presents the LLSRPSM technique and suggests some needed definitions.

In accordance with Eq (3.5), let the residual Res for the suggested PDE be expressed as

$$Res(\delta,\gamma)=\mathcal{L}^{-1}\left[\zeta(\delta,s)-\frac{f(\delta)}{s}+\frac{1}{s^{\mu}}\mathcal{L}\{N_{\delta}[\zeta(\delta,\gamma)]\}\right], \tag{3.7}$$

starting constraint

$$I(\zeta)=0. \tag{3.8}$$

Hence, the approximate solution to Eq (3.1) is represented by ζ.

Remark 3.1. $[\Im_k{}^{\mu}(\delta,s)]_{k\in N}$ *converge to the solution of Eq (3.1) if*

$$\lim_{k\to\infty}(Res(\delta,\gamma,\Im_k{}^{\mu}(\delta,\gamma)))=0. \tag{3.9}$$

Definition 3.1. *Assume that ζ is the ϵ-approximate LRPSM solution of Eq (3.1) on domain I if*

$$\left|Res(\delta,\gamma)\right|<\epsilon, \tag{3.10}$$

and ζ also satisfies Eq (3.8).

Definition 3.2. *Assume that ζ is the weak ϵ-approximate LRPSM solution of Eq (3.1) on domain I if*

$$\int\int_{I}Res^{2}(\delta,\gamma))d\delta d\gamma\leq\epsilon, \tag{3.11}$$

and ζ also satisfies Eq (3.8).

For the LLSRPSM, we suggest the following procedures.

Step 1. Using the LRPSM, we first determine the k^{th} approximate solution.

$$\zeta_k(\delta,\gamma)=\Psi_1+\Psi_2+\Psi_3+\cdots+\Psi_n. \tag{3.12}$$

Step 2. Verification of the linearly independent functions may be carried out by

$$\omega^{\mu}[\Psi_1,\Psi_2,\Psi_3\cdots,\Psi_n]=\begin{vmatrix}\Psi_1 & \Psi_2 & \Psi_3 & \cdots & \Psi_n\\ D^{\mu}\Psi_1 & D^{\mu}\Psi_2 & D^{\mu}\Psi_3 & \cdots & D^{\mu}\Psi_n\\ D^{2\mu}\Psi_1 & D^{2\mu}\Psi_2 & D^{2\mu}\Psi_3 & \cdots & D^{2\mu}\Psi_n\\ \vdots & \vdots & \vdots & \vdots & \vdots\\ D^{(n-1)\mu}\Psi_1 & D^{(n-1)\mu}\Psi_2 & D^{(n-1)\mu}\Psi_3 & \cdots & D^{(n-1)\mu}\Psi_n\end{vmatrix}\neq 0 \tag{3.13}$$

where $D^{\mu}\Psi_k=(\frac{\partial}{\partial\delta}+\frac{\partial^{\mu}}{\partial\gamma^{\mu}})\Psi_k,\ 0<\mu\leq 0$.

Assume that in the vector space of continuous functions defined on I, $S_k=\Psi_1,\Psi_2,\Psi_3,\cdots,\Psi_n$ and its components are linearly independent for $k=1,2,3,\cdots,n$.

Remark 3.2. *The set S_k is said to be linearly dependent, if there is not such a point for which $\omega^{\mu}[\Psi_1,\Psi_2,\Psi_3\cdots,\Psi_n]\neq 0$. So, we use the classical LRPSM in such a situation.*

Step 3. Consider that Eq (3.1) has the following approximate solution

$$\zeta_k = \sum_{n=0}^{k} \Upsilon_k^n \Psi_r. \tag{3.14}$$

Insert ζ_k in Eq (3.7), and we get

$$Res(\delta, \gamma, \Upsilon_k^n) = Res_k(\delta, \gamma). \tag{3.15}$$

Step 4. We attach to the subsequent functional:

$$min(J) = \int \int_I Res^2(\delta, \gamma, \Upsilon_k^n) d\delta d\gamma. \tag{3.16}$$

Here, a few constants $\Upsilon_k^{m+1}, \Upsilon_k^{m+2}, \Upsilon_k^{m+3}, \cdots, \Upsilon_k^n$ are calculated.

Using the starting conditions, we calculate the values of $\Upsilon_k^{m+1}, \Upsilon_k^{m+2}, \Upsilon_k^{m+3}, \cdots, \Upsilon_k^n$ as the values that provide the minimum of Eq (3.16) and the values of $\Upsilon_k^0, \Upsilon_k^1, \Upsilon_k^2, \cdots, \Upsilon_k^m$ as functions of $\Upsilon_k^{m+1}, \Upsilon_k^{m+2}, \Upsilon_k^{m+3}, \cdots, \Upsilon_k^n$ again.

When we solve Eq (3.16), we can obtain the values of ${\Im_k}^{\mu}(\delta, \gamma)$:

$${\Im_k}^{\mu}(\delta, \gamma) = \sum_{n=0}^{k} \Upsilon_k^n \Psi_r. \tag{3.17}$$

We may obtain the following result from Eq (3.14) to (3.17)

$$Res^2(\delta, \gamma, {\Im_k}^{\mu}) \leq {Res^2}_k(\delta, \gamma). \tag{3.18}$$

In our study, we begin by formulating the fractional partial differential equation using the Caputo derivative and then we apply the Laplace transform to convert the time-fractional derivative into an algebraic expression, thereby simplifying the problem. Next, we assume a power series expansion for the solution and substitute it into the transformed equation, which leads to a residual function that quantifies the deviation from an exact solution. To minimize this residual, we employ a least squares optimization strategy, determining the optimal coefficients in the series expansion. For the stability analysis, we introduce a small perturbation to the obtained approximate solution and express this perturbation as a Fourier mode, which allows us to derive a growth factor. The method is considered stable if this growth factor remains less than or equal to one under the chosen conditions. Finally, numerical experiments are conducted to validate that the residual error diminishes over iterations, confirming that the Laplace least squares residual power series method is robust and reliable when applied to fractional partial differential equations.

Theorem 3.3. *${\Im_k}^{\mu}(\delta, \gamma)$'s values meet the following property [59]:*

$$\lim_{k \to \infty} \int \int_I \left(Res^2(\delta, \gamma, {\Im_k}^{\mu}) \right) d\delta d\gamma = 0. \tag{3.19}$$

Proof. The subsequent inequality is based on the computation of ${\Im_k}^{\mu}(\delta, \gamma)$:

$$\int \int_I \left(Res^2(\delta, \gamma, {\Im_k}^{\mu}) \right) d\delta d\gamma \geq 0. \tag{3.20}$$

Also, from Eq (3.18), we have

$$\int\int_I \Big(Res^2{}_k(\delta,\gamma)\Big)\,d\delta d\gamma \geq \int\int_I \Big(Res^2(\delta,\gamma,\Im_k{}^\mu)\Big)\,d\delta d\gamma,\ \forall\ k \in N. \tag{3.21}$$

As the convergence of the LRPSM solution, we have

$$\begin{aligned} 0 &\leq \lim_{k\to\infty} \int\int_I \Big(Res^2(\delta,\gamma,\Im_k{}^\mu)\Big)\,d\delta d\gamma, \\ &\leq \lim_{k\to\infty} \int\int_I \Big(Res^2{}_k(\delta,\gamma)\Big)\,d\delta d\gamma = 0. \end{aligned} \tag{3.22}$$

The weak solutions of Eq (3.1) are also the ϵ-approximate residual power series solutions $\Im_k{}^\mu(\delta,\gamma)$. □

4. The general implementation of Laplace least squares variational iteration method

4.1. Laplace variation iteration transform method (LVIM)

Assume the fractional-order nonlinear PDE

$$D_\gamma^\mu \zeta(\delta,\gamma) = \mathcal{R}\zeta(\delta,\gamma) + \mathcal{N}\zeta(\delta,\gamma) + \mathbb{H}(\delta,\gamma),\ \ \mu \in (0,1]. \tag{4.1}$$

Starting constraint

$$\zeta(\delta,0) = \zeta_0(\delta). \tag{4.2}$$

Utilize the LT on Eq (4.1),

$$\mathcal{L}[D_\gamma^\mu \zeta(\delta,\gamma)] = \mathcal{L}[\mathcal{R}\zeta(\delta,\gamma) + \mathcal{N}\zeta(\delta,\gamma) + \mathbb{H}(\delta,\gamma)]. \tag{4.3}$$

By utilizing the iterative capability of the transform, the following outcome may be obtained:

$$\mathcal{L}[\zeta(\delta,\gamma)] - \sum_{k=0}^{m-1} s^{\mu-k-1} \frac{\partial^k \zeta(\delta,\gamma)}{\partial\gamma^k}|_{\gamma=0} = \mathcal{L}[\mathcal{R}\zeta(\delta,\gamma) + \mathcal{N}\zeta(\delta,\gamma) + \mathbb{H}(\delta,\gamma)]. \tag{4.4}$$

The Lagrange multiplier $(-\lambda(s))$ is used in an iterative process.

$$\mathcal{L}[\zeta_{n+1}(\delta,\gamma)] = \mathcal{L}[\zeta_n(\delta,\gamma)] - \lambda(s)\Big[\mathcal{L}[\zeta_n(\delta,\gamma)] - \sum_{k=0}^{m-1} s^{\mu-k-1} \frac{\partial^k \zeta(\delta,0)}{\partial\gamma^k}\Big]. \tag{4.5}$$

Substitute Eq (4.5) into Eq (4.4) after taking $\lambda(s) = -\frac{1}{s^\mu}$.

$$\begin{aligned} \mathcal{L}[\zeta_{n+1}(\delta,\gamma)] = \mathcal{L}[\zeta_n(\delta,\gamma)] - \lambda(s)\Big[\mathcal{L}[\zeta_n(\delta,\gamma)] - \sum_{k=0}^{m-1} s^{\mu-k-1} \frac{\partial^k \zeta(\delta,0)}{\partial\gamma^k} \\ + \mathcal{L}[\mathcal{R}\zeta(\delta,\gamma) + \mathcal{N}\zeta(\delta,\gamma) + \mathbb{H}(\delta,\gamma)]\Big]. \end{aligned} \tag{4.6}$$

Eq (4.6), using LIT, yields

$$\zeta_{n+1}(\delta,\gamma) = \zeta_n(\delta,\gamma) + \mathcal{L}^{-1}\Big[\frac{1}{s^\mu}\sum_{k=0}^{m-1} s^{\mu-k-1}\frac{\partial^k\zeta(\delta,0)}{\partial\gamma^k} + \mathcal{L}[\mathcal{R}\zeta(\delta,\gamma) + \mathcal{N}\zeta(\delta,\gamma) + \mathbb{H}(\delta,\gamma)]\Big]. \tag{4.7}$$

The following is the starting constraint:

$$\zeta_0(\delta,\gamma) = \mathcal{L}^{-1}\Big[\frac{1}{s^\mu}\sum_{k=0}^{m-1} s^{\mu-k-1}\frac{\partial^k\zeta(\delta,0)}{\partial\gamma^k}\Big]. \tag{4.8}$$

The recursive formula that is built is as follows:

$$\zeta_{n+1}(\delta,\gamma) = \zeta_n(\delta,\gamma) + \mathcal{L}^{-1}\Big[\frac{1}{s^\mu}\sum_{k=0}^{m-1} s^{\mu-k-1}\frac{\partial^k\zeta(\delta,0)}{\partial\gamma^k} + \mathcal{L}[\mathcal{R}\zeta(\delta,\gamma) + \mathcal{N}\zeta(\delta,\gamma) + \mathbb{H}(\delta,\gamma)]\Big]. \tag{4.9}$$

4.2. Laplace least squares variational iteration method (LLSVIM)

The procedure of the LLSVIM method is presented in this section.
Let us express the remainder $\Re_{LVIM}$ for the suggested PDE using Equation 4.1 as

$$\Re_{LVIM_{k+1}}(\delta,\gamma) = \zeta_k(\delta,\gamma) + \mathcal{L}^{-1}\Big[\frac{1}{s^\mu}\sum_{\kappa=0}^{m-1} s^{\mu-\kappa-1}\frac{\partial^\kappa\zeta(\delta,0)}{\partial\gamma^\kappa} + \mathcal{L}[\mathcal{R}\zeta(\delta,\gamma) + \mathcal{N}\zeta(\delta,\gamma) + \mathbb{H}(\delta,\gamma)]\Big], \tag{4.10}$$

starting constraint

$$I(\zeta) = 0. \tag{4.11}$$

The approximate solution of Eq (4.1) is represented by ζ.
Step 1. First, we use LVIM to obtain the k^{th} approximate solution.

$$\zeta_k(\delta,\gamma) = \Psi_1 + \Psi_2 + \Psi_3 + \cdots + \Psi_n. \tag{4.12}$$

Step 2. Verification of the linearly independent functions may be carried out by

$$\omega^\mu[\Psi_1,\Psi_2,\Psi_3\cdots,\Psi_n] = \begin{vmatrix} \Psi_1 & \Psi_2 & \Psi_3 & \cdots & \Psi_n \\ D^\mu\Psi_1 & D^\mu\Psi_2 & D^\mu\Psi_3 & \cdots & D^\mu\Psi_n \\ D^{2\mu}\Psi_1 & D^{2\mu}\Psi_2 & D^{2\mu}\Psi_3 & \cdots & D^{2\mu}\Psi_n \\ \vdots & \vdots & \vdots & \vdots & \vdots \\ D^{(n-1)\mu}\Psi_1 & D^{(n-1)\mu}\Psi_2 & D^{(n-1)\mu}\Psi_3 & \cdots & D^{(n-1)\mu}\Psi_n \end{vmatrix} \neq 0 \tag{4.13}$$

where $D^\mu\Psi_k = (\frac{\partial}{\partial\delta} + \frac{\partial^\mu}{\partial\gamma^\mu})\Psi_k,\ 0 < \mu \leq 0$.

Assume that in the vector space of continuous functions defined on I, $S_k = \Psi_1,\Psi_2,\Psi_3,\cdots,\Psi_n$ and its components are linearly independent for $k = 1,2,3,\cdots,n$.
Step 3. Assume the subsequent approximate solution to Eq (4.1):

$$\zeta_k = \sum_{n=0}^{k} \Upsilon_k^n\Psi_r. \tag{4.14}$$

Insert ζ_k in Eq (4.10), we get

$$\Re_{LVIM}(\delta, \gamma, \Upsilon_k^n) = \Re_{LVIM_k}(\delta, \gamma). \tag{4.15}$$

Step 4. We attach to the subsequent functional:

$$min(J) = \int \int_I \Re_{LVIM}{}^2(\delta, \gamma, \Upsilon_k^n) d\delta d\gamma. \tag{4.16}$$

The constants Υ_k^n are calculated using Eq (4.16) and then the values of these constants are put in Eq (4.14) to obtain the LLSVIM approximate solution.

5. Numerical example 1

5.1. Implementation of LLSRPSM

Consider the fractional damped Burgers' equation

$$D_\gamma^\mu \zeta(\delta, \gamma) + \frac{\partial^2 \zeta(\delta, \gamma)}{\partial \delta^2} + \zeta(\delta, \gamma) \frac{\partial \zeta(\delta, \gamma)}{\partial \delta} + \frac{1}{5} \zeta(\delta, \gamma) = 0, \ \gamma > 0, \ 0 < \mu \leq 1, \tag{5.1}$$

starting constraint

$$\zeta(\delta, 0) = \frac{\delta}{5}. \tag{5.2}$$

Using the LRPSM, we get

$$\begin{aligned} \Psi_0 &= \frac{\delta}{5}, \\ \Psi_1 &= -\frac{2\delta\gamma^\mu}{25\Gamma(\mu+1)}, \\ \Psi_2 &= \frac{6\delta\gamma^{2\mu}}{125\Gamma(2\mu+1)}. \end{aligned} \tag{5.3}$$

Then,

$$\omega^\mu[\Psi_0, \Psi_1, \Psi_2] = \begin{vmatrix} \frac{\delta}{5} & -\frac{2\delta\gamma^\mu}{25\Gamma(\mu+1)} & \frac{6\delta\gamma^{2\mu}}{125\Gamma(2\mu+1)} \\ D^\mu\left(\frac{\delta}{5}\right) & D^\mu\left(-\frac{2\delta\gamma^\mu}{25\Gamma(\mu+1)}\right) & D^\mu\left(\frac{6\delta\gamma^{2\mu}}{125\Gamma(2\mu+1)}\right) \\ D^{2\mu}\left(\frac{\delta}{5}\right) & D^{2\mu}\left(-\frac{2\delta\gamma^\mu}{25\Gamma(\mu+1)}\right) & D^{2\mu}\left(\frac{6\delta\gamma^{2\mu}}{125\Gamma(2\mu+1)}\right) \end{vmatrix}. \tag{5.4}$$

When $\mu = 1$, $\delta = 15$, and $\gamma = 0.5$, $\omega^1[\Psi_0, \Psi_1, \Psi_2] = -2.592 \neq 0$. Hence, the functions Ψ_0, Ψ_1, and Ψ_2 are linearly independent.

This allows us to derive the approximate solution, which is expressed as

$$\zeta(\delta, \gamma) = \Upsilon_0\left(\frac{\delta}{5}\right) + \Upsilon_1\left(-\frac{2\delta\gamma^\mu}{25\Gamma(\mu+1)}\right) + \Upsilon_2\left(\frac{6\delta\gamma^{2\mu}}{125\Gamma(2\mu+1)}\right). \tag{5.5}$$

Equation (5.1) provides the residual function.

$$Res(\delta, \gamma) = D_\gamma^\mu \zeta(\delta, \gamma) + \frac{\partial^2 \zeta(\delta, \gamma)}{\partial \delta^2} + \zeta(\delta, \gamma) \frac{\partial \zeta(\delta, \gamma)}{\partial \delta} + \frac{1}{5} \zeta(\delta, \gamma), \tag{5.6}$$

with the starting constraint

$$\zeta(\delta, 0) = \frac{\delta}{5}. \tag{5.7}$$

$\Upsilon_0 = 1$ is obtained by applying the specified condition Eq (5.7) in Eq (5.5). Therefore, Eq (5.5) may be expressed as

$$\zeta(\delta, \gamma) = \frac{\delta}{5} + \Upsilon_1\left(-\frac{2\delta\gamma^{\mu}}{25\Gamma(\mu+1)}\right) + \Upsilon_2\left(\frac{6\delta\gamma^{2\mu}}{125\Gamma(2\mu+1)}\right). \tag{5.8}$$

In this way, we may get Res by putting Eq (5.8) in Eq (5.6). Hence, the functional J will be

$$J(\Upsilon_1, \Upsilon_2) = \int\int_I Res^2(\delta, \gamma, \Upsilon_k) d\delta d\gamma, \ \textit{where } k = 1, 2. \tag{5.9}$$

We calculate the minimal of J in Eq (5.9) and obtain two algebraic equations,

$$\begin{aligned} \frac{\partial J}{\partial \Upsilon_1} &= 0, \\ \frac{\partial J}{\partial \Upsilon_2} &= 0. \end{aligned} \tag{5.10}$$

Hence, when $\mu = 1$, we obtain the unknown coefficients of Eq (5.10):

$$\begin{aligned} \Upsilon_1 &= 0.9995859373898288, \\ \Upsilon_2 &= 0.9581200433133302. \end{aligned} \tag{5.11}$$

Putting the values of Eq (5.11) in Eq (5.8), we get the LLSRPSM solution.

For $\mu = 1$, the exact solution is given as

$$\zeta(\delta, \gamma) = \frac{\delta}{5\left(2e^{\frac{\gamma}{5}} - 1\right)}. \tag{5.12}$$

5.2. Implementation of LLSVIM

Consider the fractional damped Burgers' equation

$$D_{\gamma}^{\mu}\zeta(\delta, \gamma) + \frac{\partial^2\zeta(\delta, \gamma)}{\partial\delta^2} + \zeta(\delta, \gamma)\frac{\partial\zeta(\delta, \gamma)}{\partial\delta} + \frac{1}{5}\zeta(\delta, \gamma) = 0, \ \gamma > 0, \ 0 < \mu \leq 1, \tag{5.13}$$

starting constraint

$$\zeta(\delta, 0) = \frac{\delta}{5}, \tag{5.14}$$

Using the LVIM, we get

$$\begin{aligned} \Psi_0 &= \frac{\delta}{5}, \\ \Psi_1 &= -\frac{2\delta\gamma^{\mu}}{25\Gamma(\mu+1)}, \\ \Psi_2 &= \frac{6\delta\gamma^{2\mu}}{125\Gamma(2\mu+1)} - \frac{4\delta\Gamma(2\mu+1)\gamma^{3\rho}}{625\Gamma(\mu+1)^2\Gamma(3\mu+1)}. \end{aligned} \tag{5.15}$$

Then,

$$\omega^{\mu}[\Psi_0,\Psi_1,\Psi_2]=\begin{vmatrix} \frac{\delta}{5} & -\frac{2\delta\gamma^{\mu}}{25\Gamma(\mu+1)} & \frac{6\delta\gamma^{2\mu}}{125\Gamma(2\mu+1)}-\frac{4\delta\Gamma(2\mu+1)\gamma^{3\rho}}{625\Gamma(\mu+1)^2\Gamma(3\mu+1)} \\ D^{\mu}\left(\frac{\delta}{5}\right) & D^{\mu}\left(-\frac{2\delta\gamma^{\mu}}{25\Gamma(\mu+1)}\right) & D^{\mu}\left(\frac{6\delta\gamma^{2\mu}}{125\Gamma(2\mu+1)}-\frac{4\delta\Gamma(2\mu+1)\gamma^{3\rho}}{625\Gamma(\mu+1)^2\Gamma(3\mu+1)}\right) \\ D^{2\mu}\left(\frac{\delta}{5}\right) & D^{2\mu}\left(-\frac{2\delta\gamma^{\mu}}{25\Gamma(\mu+1)}\right) & D^{2\mu}\left(\frac{6\delta\gamma^{2\mu}}{125\Gamma(2\mu+1)}-\frac{4\delta\Gamma(2\mu+1)\gamma^{3\rho}}{625\Gamma(\mu+1)^2\Gamma(3\mu+1)}\right) \end{vmatrix}. \tag{5.16}$$

When $\mu=1$, $\delta=15$, and $\gamma=0.5$, $\omega^{1}[\Psi_0,\Psi_1,\Psi_2]=-2.2464\neq 0$. Hence, the functions Ψ_0, Ψ_1, and Ψ_2 are linearly independent.

This allows us to derive the approximate solution, which is expressed as

$$\zeta(\delta,\gamma)=\Upsilon_0\left(\frac{\delta}{5}\right)+\Upsilon_1\left(-\frac{2\delta\gamma^{\mu}}{25\Gamma(\mu+1)}\right)+\Upsilon_2\left(\frac{6\delta\gamma^{2\mu}}{125\Gamma(2\mu+1)}-\frac{4\delta\Gamma(2\mu+1)\gamma^{3\rho}}{625\Gamma(\mu+1)^2\Gamma(3\mu+1)}\right). \tag{5.17}$$

Equation (5.13) provides the residual function.

$$\Re_{LVIM}(\delta,\gamma)=D^{\mu}_{\gamma}\zeta(\delta,\gamma)+\frac{\partial^2\zeta(\delta,\gamma)}{\partial\delta^2}+\zeta(\delta,\gamma)\frac{\partial\zeta(\delta,\gamma)}{\partial\delta}+\frac{1}{5}\zeta(\delta,\gamma), \tag{5.18}$$

with the starting constraint

$$\zeta(\delta,0)=\frac{\delta}{5}. \tag{5.19}$$

$\Upsilon_0=1$ is obtained by applying the specified condition of Eq (5.19) in Eq (5.17). Therefore, Eq (5.17) may be expressed as

$$\zeta(\delta,\gamma)=\frac{\delta}{5}+\Upsilon_1\left(-\frac{2\delta\gamma^{\mu}}{25\Gamma(\mu+1)}\right)+\Upsilon_2\left(\frac{6\delta\gamma^{2\mu}}{125\Gamma(2\mu+1)}-\frac{4\delta\Gamma(2\mu+1)\gamma^{3\rho}}{625\Gamma(\mu+1)^2\Gamma(3\mu+1)}\right). \tag{5.20}$$

In this way, we may get $\Re_{LVIM}$ by putting Eq (5.20) in Eq (5.18). Hence, the functional J will be

$$J(\Upsilon_1,\Upsilon_2)=\int\int_I {\Re_{LVIM}}^2(\delta,\gamma,\Upsilon_k)d\delta d\gamma,\ \textit{where } k=1,2. \tag{5.21}$$

We compute the functional J of Eq (5.21). We receive two algebraic equations as

$$\frac{\partial J}{\partial\Upsilon_1}=0,\frac{\partial J}{\partial\Upsilon_2}=0. \tag{5.22}$$

Hence, when $\mu=1$, we obtain the unknown coefficients of Eq (5.22):

$$\Upsilon_1=0.9997161819861972,\Upsilon_2=0.9710931448883657. \tag{5.23}$$

Putting the values of Eq (5.23) in Eq (5.20), we get the LLSVIM solution.

The analysis combines various graphical illustrations with tabulated results to study solutions derived through LLSRPSM and LLSVIM. The proposed methods require visual and numerical data to show their accuracy and confirm convergence and behavior across different fractional orders.

Figure 1 illustrates the fractional solutions that LLSRPSM produces when implementing fractional parameter values μ during the computation process. The figure shows solution characteristics at $\mu = 0.5$ in subfigure (a) with additional visualizations at $\mu = 0.7$ in subfigure (b), and $\mu = 1.0$ in subfigure (c). The combined solution comparison at $\mu = 0.5, 0.7$, and 1.0 is given in subfigure (d) when $\gamma = 0.1$. The experimental results demonstrate how different fractional orders impact the shape along with stability characteristics of obtained solutions.

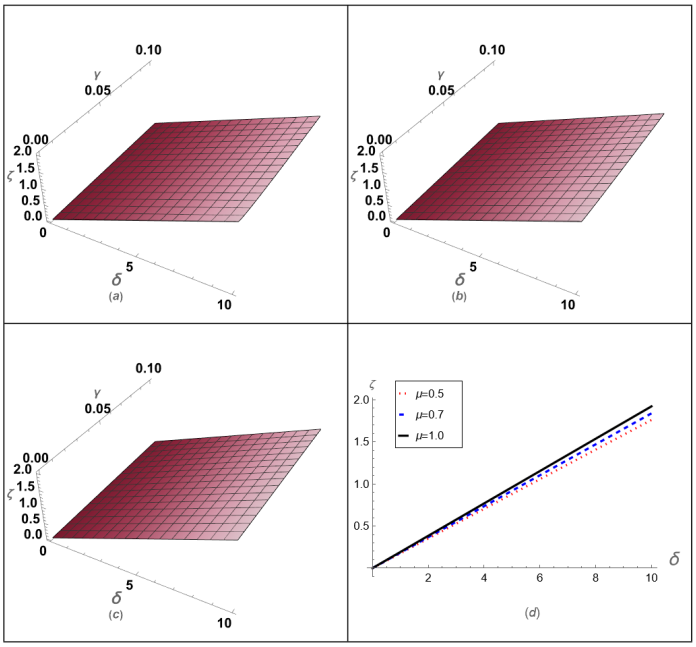

Figure 1. (a) LLSRPSM solution for $\mu = 0.5$; (b) LLSRPSM solution for $\mu = 0.7$; (c) LLSRPSM solution for $\mu = 1.0$; (d) LLSRPSM solution comparison for $\mu = 0.5, 0.7$, and 1.0 at $\gamma = 0.1$.

The LLSRPSM solution shown in Figure 2 matches the exact analytical solution when μ equals 1.0 and γ equals 0.1, which proves the accuracy of this proposed technique. Visual verification of the two solutions through comparison confirms the dependable and effective nature of the LLSRPSM method.

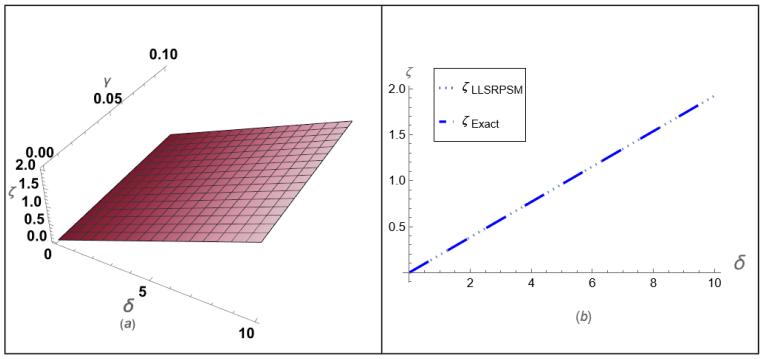

Figure 2. The LLRPSM solution and exact solution comparison for $\mu = 1.0$ and $\gamma = 0.1$.

Figure 3 showcases three-dimensional fractional-order LLSRPSM solutions at $\gamma = 0.1$ for the four values of μ: 0.3, 0.5, 0.7, and 1.0. The illustrations show the solution structure transformation as

fractional orders transform indicating that the fractional model functions dynamically.

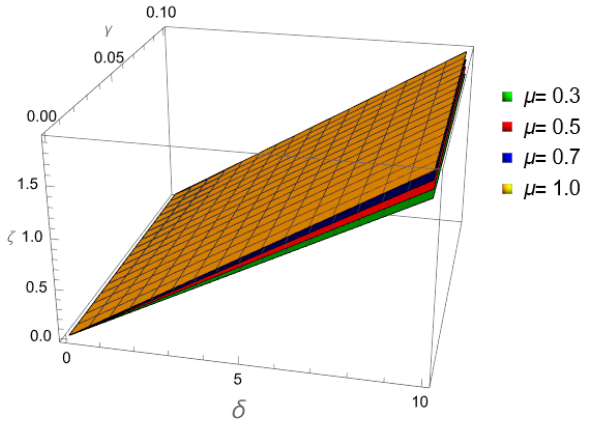

Figure 3. The 3D fractional-order comparison for $\mu = 0.3, 0.5, 0.7$, and 1.0 for $\gamma = 0.1$.

The results produced by LLSVIM appear in Figure 4 with an organization matching the format of Figure 1. Figure 4 shows the effect of different fractional orders ($\mu = 0.5, 0.7, 1.0$) on the results presented in subfigure (d) at $\gamma = 0.1$. The performance assessment of the method becomes possible through direct analysis of its fractional-order configurations in different settings.

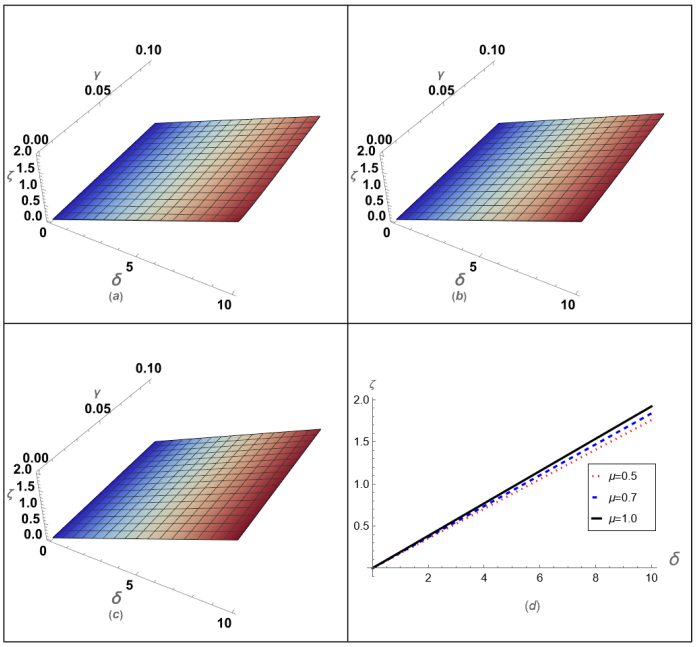

Figure 4. (a) LLSVIM solution for $\mu = 0.5$; (b) LLSVIM solution for $\mu = 0.7$; (c) LLSVIM solution for $\mu = 1.0$; (d) LLSVIM solution comparison for $\mu = 0.5, 0.7$, and 1.0 at $\gamma = 0.1$.

The LLSVIM solution matches exactly with the exact solution at a μ value of 1.0 and γ value of 0.1, as shown in Figure 5. The performance of LLSVIM becomes evident because it provides accurate approximations of analytical solutions. A 3D fractional-order representation at $\gamma = 0.1$ comparing $\mu = 0.3, 0.5, 0.7$, and 1.0 appears in Figure 6 following LLSVIM. The fractional-order

solution simulations in the results shed more light on how the method measures up against the system dynamics.

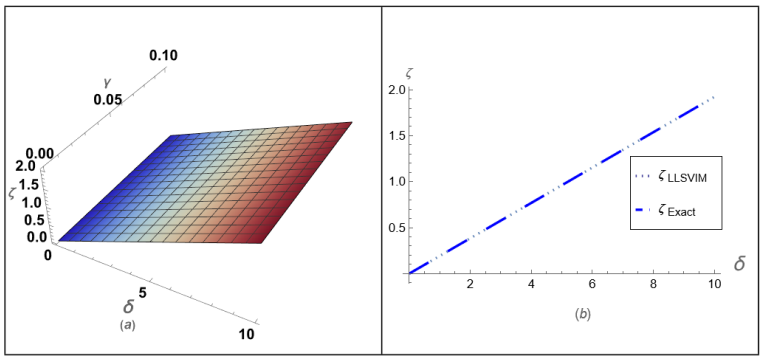

Figure 5. The LLRVIM solution and exact solution comparison for $\mu = 1.0$ and $\gamma = 0.1$.

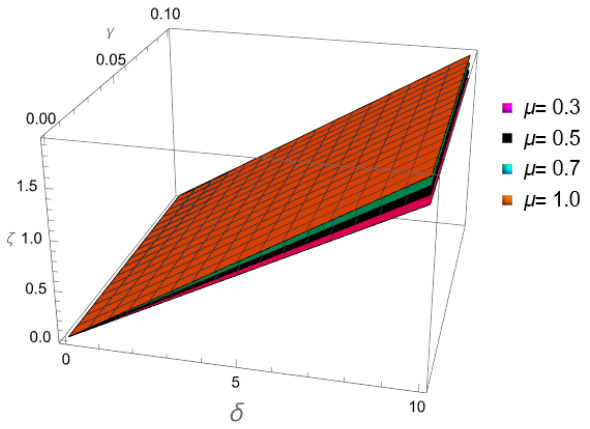

Figure 6. The 3D fractional-order comparison for $\mu = 0.3, 0.5, 0.7$, and 1.0 for $\gamma = 0.1$.

The provided Table 1 displays the fractional-order solution $\zeta(\delta, \gamma)$ evaluated at $\gamma = 0.10$ through LRPSM and LLSRPSM for the numerical example 1. The proposed method shows its accuracy and convergence performance through these numerical values when used for different fractional orders. The fractional-order evaluation of solution $\zeta(\delta, \gamma)$ at $\gamma = 0.10$ comes from LVIM and LLSVIM methods for the numerical example 1 as shown in Table 2. The variational iteration-based approach demonstrates high effectiveness in solving fractional differential equations according to the presented results. The solutions from LLSRPSM and LLSVIM at a γ value of 0.10 are examined in Table 3 regarding the numerical example 1. The analysis enables a broader assessment of method suitability through a presentation of their combined advantages and weaknesses. These research methods demonstrate powerful performance in dealing with fractional nonlinear differential equations based on the presented figures and tables. These techniques demonstrate remarkable accuracy in their ability to solve nonlinear fractional models as proven through both exact solution checking and numerical validation processes for mathematical physics and engineering applications.

Table 1. The fractional-order analysis of the solution $\zeta(\delta,\gamma)$ at $\gamma = 0.10$ obtained through $LRPSM$ and $LLSRPSM$ absolute error (AE) for numerical example 1.

	$\mu = 0.7$	$\mu = 0.7$	$\mu = 1.0$	$\mu = 1.0$		$\mu = 1.0$	$\mu = 1.0$
δ	$\zeta(\delta,\gamma)_{LRPSM}$	$\zeta(\delta,\gamma)_{LLSRPSM}$	$\zeta(\delta,\gamma)_{LRPSM}$	$\zeta(\delta,\gamma)_{LLSRPSM}$	$Exact$	AE of LRPSM	AE of LLSRPSM
1	0.18397132	0.18391416	0.19224000	0.19223326	0.19223326	6.73894216×10^{-6}	2.53439519×10^{-10}
2	0.36794264	0.36782833	0.38448000	0.38446652	0.38446652	1.34778843×10^{-5}	5.06879038×10^{-10}
3	0.55191396	0.55174250	0.57672000	0.57669978	0.57669978	2.02168264×10^{-5}	7.60318474×10^{-10}
4	0.73588529	0.73565667	0.76896000	0.76893304	0.76893304	2.69557686×10^{-5}	1.01375807×10^{-9}
5	0.91985661	0.91957084	0.96119999	0.96116630	0.96116630	3.36947108×10^{-5}	1.26719756×10^{-9}
6	1.10382793	1.10348501	1.15344000	1.15339956	1.15339956	4.04336529×10^{-5}	1.52063694×10^{-9}
7	1.28779925	1.28739918	1.34567999	1.34563282	1.34563282	4.71725951×10^{-5}	1.77407644×10^{-9}
8	1.47177058	1.47131335	1.53792000	1.53786609	1.53786608	5.39115373×10^{-5}	2.02751615×10^{-9}
9	1.65574190	1.65522752	1.73016000	1.73009935	1.73009934	6.06504794×10^{-5}	2.28095564×10^{-9}
10	1.83971322	1.83914169	1.92239999	1.92233261	1.92233261	6.73894216×10^{-5}	2.53439513×10^{-9}

Table 2. The fractional-order analysis of the solution $\zeta(\delta,\gamma)$ at $\gamma = 0.10$ obtained through $LVIM$ and $LLSVIM$ for numerical example 1.

	$\mu = 0.7$	$\mu = 0.7$	$\mu = 1.0$	$\mu = 1.0$		$\mu = 1.0$	$\mu = 1.0$
δ	$\zeta(\delta,\gamma)_{LVIM}$	$\zeta(\delta,\gamma)_{LLSVIM}$	$\zeta(\delta,\gamma)_{LVIM}$	$\zeta(\delta,\gamma)_{LLSVIM}$	$Exact$	AE of LVIM	AE of LLSVIM
1	0.18393651	0.18389804	0.19223786	0.19223326	0.19223326	4.60560882×19^{-6}	1.75670811×19^{-10}
2	0.36787303	0.36779608	0.38447573	0.38446652	0.38446652	9.21121765×19^{-6}	3.51341622×19^{-10}
3	0.55180955	0.55169412	0.57671359	0.57669978	0.57669978	1.38168264×19^{-5}	5.27012322×19^{-10}
4	0.73574607	0.73559216	0.76895146	0.76893304	0.76893304	1.84224353×19^{-5}	7.02683244×19^{-10}
5	0.91968259	0.91949020	0.96118933	0.96116630	0.96116630	2.30280441×19^{-5}	8.78354167×19^{-10}
6	1.10361911	1.10338824	1.15342719	1.15339956	1.15339956	2.76336529×19^{-5}	1.05402464×19^{-9}
7	1.28755563	1.28728628	1.34566506	1.34563282	1.34563282	3.22392618×19^{-5}	1.22969567×19^{-9}
8	1.47149215	1.47118433	1.53790293	1.53786608	1.53786608	3.68448706×19^{-5}	1.40536648×19^{-9}
9	1.65542866	1.65508237	1.73014080	1.73009935	1.73009934	4.14504794×19^{-5}	1.58103752×19^{-9}
10	1.83936518	1.83898041	1.92237866	1.92233261	1.92233261	4.60560882×19^{-5}	1.75670833×19^{-9}

Table 3. The comparison of LLSRPSM and LLSVIM solutions $\zeta(\delta,\gamma)$ at $\gamma = 0.10$ for numerical example 1.

δ	$\zeta(\delta,\gamma)_{LLSRPSM_{\mu=1.0}}$	$\zeta(\delta,\gamma)_{LLSVIM_{\mu=1.0}}$	$Exact$	AE LLSRPSM at $\mu = 1.0$	AE LLSVIM at $\mu = 1.0$
1	0.19223326	0.19223326	0.19223326	2.53439519×10^{-10}	1.75670811×10^{-10}
2	0.38446652	0.38446652	0.38446652	5.06879038×10^{-10}	3.51341622×10^{-10}
3	0.57669978	0.57669978	0.57669978	7.60318474×10^{-10}	5.27012322×10^{-10}
4	0.76893304	0.76893304	0.76893304	1.01375807×10^{-9}	7.02683244×10^{-10}
5	0.96116630	0.96116630	0.96116630	1.26719756×10^{-9}	8.78354167×10^{-10}
6	1.15339956	1.15339956	1.15339956	1.52063694×10^{-9}	1.05402464×10^{-9}
7	1.34563282	1.34563282	1.34563282	1.77407644×10^{-9}	1.22969567×10^{-9}
8	1.53786609	1.53786608	1.53786608	2.02751615×10^{-9}	1.40536648×10^{-9}
9	1.73009935	1.73009935	1.73009934	2.28095564×10^{-9}	1.58103752×10^{-9}
10	1.92233261	1.92233261	1.92233261	2.53439513×10^{-9}	1.75670833×10^{-9}

6. Numerical example 2

6.1. Implementation of LLSRPSM

Consider the fractional Rosenau-Hyman equation

$$D_{\gamma}^{\mu}\zeta(\delta,\gamma)-\zeta(\delta,\gamma)\frac{\partial\zeta(\delta,\gamma)}{\partial\delta}-\zeta(\delta,\gamma)\frac{\partial^{3}\zeta(\delta,\gamma)}{\partial\delta^{3}}-3\frac{\partial\zeta(\delta,\gamma)}{\partial\delta}\frac{\partial^{2}\zeta(\delta,\gamma)}{\partial\delta^{2}}=0,\ \gamma>0,\ 0<\mu\leq 1, \tag{6.1}$$

starting constraint

$$\zeta(\delta,0)=-\frac{8q}{3}\cos^{2}\left(\frac{\delta}{4}\right). \tag{6.2}$$

Utilizing LRPSM, we get

$$\begin{aligned}\Psi_{0}&=-\frac{8q}{3}\cos^{2}\left(\frac{\delta}{4}\right),\\ \Psi_{1}&=-\frac{2q^{2}\gamma^{\mu}\sin\left(\frac{\delta}{2}\right)}{3\Gamma(\mu+1)},\\ \Psi_{2}&=\frac{q^{3}\gamma^{2\mu}\cos\left(\frac{\delta}{2}\right)}{3\Gamma(2\mu+1)}.\end{aligned} \tag{6.3}$$

Then,

$$\omega^{\mu}[\Psi_{0},\Psi_{1},\Psi_{2}]=\begin{vmatrix}-\frac{8q}{3}\cos^{2}\left(\frac{\delta}{4}\right) & -\frac{2q^{2}\gamma^{\mu}\sin\left(\frac{\delta}{2}\right)}{3\Gamma(\mu+1)} & \frac{q^{3}\gamma^{2\mu}\cos\left(\frac{\delta}{2}\right)}{3\Gamma(2\mu+1)}\\ D^{\mu}\left(-\frac{8q}{3}\cos^{2}\left(\frac{\delta}{4}\right)\right) & D^{\mu}\left(-\frac{2q^{2}\gamma^{\mu}\sin\left(\frac{\delta}{2}\right)}{3\Gamma(\mu+1)}\right) & D^{\mu}\left(\frac{q^{3}\gamma^{2\mu}\cos\left(\frac{\delta}{2}\right)}{3\Gamma(2\mu+1)}\right)\\ D^{2\mu}\left(-\frac{8q}{3}\cos^{2}\left(\frac{\delta}{4}\right)\right) & D^{2\mu}\left(-\frac{2q^{2}\gamma^{\mu}\sin\left(\frac{\delta}{2}\right)}{3\Gamma(\mu+1)}\right) & D^{2\mu}\left(\frac{q^{3}\gamma^{2\mu}\cos\left(\frac{\delta}{2}\right)}{3\Gamma(2\mu+1)}\right)\end{vmatrix}. \tag{6.4}$$

When $\mu=1$, $\delta=105$, $\gamma=0.1$, and $q=1.5$, $\omega^{1}[\Psi_{0},\Psi_{1},\Psi_{2}]=-1.11836\neq 0$. Hence, the functions Ψ_{0},Ψ_{1}, and Ψ_{2} are linearly independent.

This allows us to derive the approximate solution, which is expressed as

$$\zeta(\delta,\gamma)=\Upsilon_{0}\left(-\frac{8q}{3}\cos^{2}\left(\frac{\delta}{4}\right)\right)+\Upsilon_{1}\left(-\frac{2q^{2}\gamma^{\mu}\sin\left(\frac{\delta}{2}\right)}{3\Gamma(\mu+1)}\right)+\Upsilon_{2}\left(\frac{q^{3}\gamma^{2\mu}\cos\left(\frac{\delta}{2}\right)}{3\Gamma(2\mu+1)}\right). \tag{6.5}$$

Equation (6.1) provides the residual function.

$$Res(\delta,\gamma)=D_{\gamma}^{\mu}\zeta(\delta,\gamma)-\zeta(\delta,\gamma)\frac{\partial\zeta(\delta,\gamma)}{\partial\delta}-\zeta(\delta,\gamma)\frac{\partial^{3}\zeta(\delta,\gamma)}{\partial\delta^{3}}-3\frac{\partial\zeta(\delta,\gamma)}{\partial\delta}\frac{\partial^{2}\zeta(\delta,\gamma)}{\partial\delta^{2}}, \tag{6.6}$$

with the starting constraint

$$\zeta(\delta,0)=-\frac{8q}{3}\cos^{2}\left(\frac{\delta}{4}\right). \tag{6.7}$$

$\Upsilon_0 = 1$ is obtained by applying the specified condition Eq (6.7) in Eq (6.5). Therefore, Eq (6.5) may be expressed as

$$\zeta(\delta,\gamma) = -\frac{8q}{3}\cos^2\left(\frac{\delta}{4}\right) + \Upsilon_1\left(-\frac{2q^2\gamma^\mu \sin\left(\frac{\delta}{2}\right)}{3\Gamma(\mu+1)}\right) + \Upsilon_2\left(\frac{q^3\gamma^{2\mu}\cos\left(\frac{\delta}{2}\right)}{3\Gamma(2\mu+1)}\right). \tag{6.8}$$

In this way, we may get Res by putting Eq (6.8) in Eq (6.6). Hence, the functional J will be

$$J(\Upsilon_1,\Upsilon_2) = \int\int_I Res^2(\delta,\gamma,\Upsilon_k)d\delta d\gamma, \ \textit{where } k = 1,2. \tag{6.9}$$

We compute the functional J of Eq (6.9). We receive two algebraic equations as

$$\frac{\partial J}{\partial \Upsilon_1} = 0, \ \ \frac{\partial J}{\partial \Upsilon_2} = 0. \tag{6.10}$$

Hence, when $\mu = 1$, we obtain the unknown coefficients of Eq (6.10):

$$\Upsilon_1 = 0.9990707576494097, \ \ \Upsilon_2 = 1.0005136662458496. \tag{6.11}$$

Putting the values of Eq (6.11) in Eq (6.8), we get the LLSRPSM solution.

For $\mu = 1$, the exact solution is given as

$$\zeta(\delta,\gamma) = -\frac{8q}{3}\cos^2\left(\frac{\delta - q\gamma}{4}\right). \tag{6.12}$$

6.2. Implementation of LLSVIM

Consider the fractional Rosenau-Hyman equation

$$D^\mu_\gamma\zeta(\delta,\gamma) - \zeta(\delta,\gamma)\frac{\partial\zeta(\delta,\gamma)}{\partial\delta} - \zeta(\delta,\gamma)\frac{\partial^3\zeta(\delta,\gamma)}{\partial\delta^3} - 3\frac{\partial\zeta(\delta,\gamma)}{\partial\delta}\frac{\partial^2\zeta(\delta,\gamma)}{\partial\delta^2} = 0, \ \gamma > 0, \ 0 < \mu \le 1, \tag{6.13}$$

starting constraint

$$\zeta(\delta,0) = -\frac{8q}{3}\cos^2\left(\frac{\delta}{4}\right). \tag{6.14}$$

Utilizing LVIM, we get

$$\begin{aligned}
\Psi_0 &= -\frac{8q}{3}\cos^2\left(\frac{\delta}{4}\right),\\
\Psi_1 &= -\frac{2q^2\gamma^\mu \sin\left(\frac{\delta}{2}\right)}{3\Gamma(\mu+1)},\\
\Psi_2 &= \frac{q^3\gamma^{2\rho}\cos\left(\frac{\delta}{2}\right)\cos^2\left(\frac{\delta}{4}\right)}{3\Gamma(2\mu+1)} + \frac{q^3\gamma^{2\mu}\sin^2\left(\frac{\delta}{4}\right)\cos\left(\frac{\delta}{2}\right)}{3\Gamma(2\mu+1)}.
\end{aligned} \tag{6.15}$$

Then,

$$\omega^\mu[\Psi_0,\Psi_1,\Psi_2] = \begin{vmatrix} \Psi_0 & \Psi_1 & \Psi_2 \\ D^\mu\Psi_0 & D^\mu\Psi_1 & D^\mu\Psi_2 \\ D^{2\mu}\Psi_0 & D^{2\mu}\Psi_1 & D^{2\mu}\Psi_2 \end{vmatrix}. \tag{6.16}$$

When $\mu = 1$, $\delta = 105$, $\gamma = 0.1$, and $q = 1.5$, $\omega^1[\Psi_0, \Psi_1, \Psi_2] = -1.11836 \neq 0$. Hence, the functions Ψ_0, Ψ_1, and Ψ_2 are linearly independent.

This allows us to derive the approximate solution, which is expressed as

$$\zeta(\delta,\gamma) = \Upsilon_0\left(-\frac{8q}{3}\cos^2\left(\frac{\delta}{4}\right)\right) + \Upsilon_1\left(-\frac{2q^2\gamma^\mu \sin\left(\frac{\delta}{2}\right)}{3\Gamma(\mu+1)}\right) + \Upsilon_2\Big(\frac{q^3\gamma^{2\rho}\cos\left(\frac{\delta}{2}\right)\cos^2\left(\frac{\delta}{4}\right)}{3\Gamma(2\mu+1)} + \frac{q^3\gamma^{2\mu}\sin^2\left(\frac{\delta}{4}\right)\cos\left(\frac{\delta}{2}\right)}{3\Gamma(2\mu+1)}\Big) \tag{6.17}$$

Eq (6.13) provides the residual function.

$$\Re_{LVIM}(\delta,\gamma) = D^\mu_\gamma\zeta(\delta,\gamma) - \zeta(\delta,\gamma)\frac{\partial\zeta(\delta,\gamma)}{\partial\delta} - \zeta(\delta,\gamma)\frac{\partial^3\zeta(\delta,\gamma)}{\partial\delta^3} - 3\frac{\partial\zeta(\delta,\gamma)}{\partial\delta}\frac{\partial^2\zeta(\delta,\gamma)}{\partial\delta^2}, \tag{6.18}$$

with the starting constraint

$$\zeta(\delta,0) = -\frac{8q}{3}\cos^2\left(\frac{\delta}{4}\right). \tag{6.19}$$

$\Upsilon_0 = 1$ is obtained by applying the specified condition Eq (6.19) in Eq (6.17). Therefore, Eq (6.17) may be expressed as

$$\begin{aligned}\zeta(\delta,\gamma) = -\frac{8q}{3}\cos^2\left(\frac{\delta}{4}\right) + \Upsilon_1\left(-\frac{2q^2\gamma^\mu \sin\left(\frac{\delta}{2}\right)}{3\Gamma(\mu+1)}\right)\\ + \Upsilon_2\Big(\frac{q^3\gamma^{2\rho}\cos\left(\frac{\delta}{2}\right)\cos^2\left(\frac{\delta}{4}\right)}{3\Gamma(2\mu+1)} + \frac{q^3\gamma^{2\mu}\sin^2\left(\frac{\delta}{4}\right)\cos\left(\frac{\delta}{2}\right)}{3\Gamma(2\mu+1)}\Big).\end{aligned} \tag{6.20}$$

In this way, we may get $\Re_{LVIM}$ by putting Eq (6.20) in Eq (6.18). Hence, the functional J will be

$$J(\Upsilon_1,\Upsilon_2) = \int\int_I {\Re_{LVIM}}^2(\delta,\gamma,\Upsilon_k)d\delta d\gamma, \ \textit{where } k = 1,2. \tag{6.21}$$

We compute the functional J of Eq (6.21). We receive two algebraic equations as

$$\frac{\partial J}{\partial\Upsilon_1} = 0, \ \ \frac{\partial J}{\partial\Upsilon_2} = 0, \tag{6.22}$$

Hence, when $\mu = 1$, we obtain the unknown coefficients of Eq (6.22):

$$\Upsilon_1 = 0.999070757649409, \ \ \Upsilon_2 = 1.000513666245874. \tag{6.23}$$

Putting the values of Eq (6.23) in Eq (6.20), we get the LLSVIM solution.

A graphical and tabulated display serves as an effective method to validate the approximate solutions derived using multiple methods for solving the fractional-order nonlinear model. These visual displays, together with numerical figures, reveal essential information about solution behavior at different fractional orders, which helps confirm the accuracy of the proposed solution methods.

The selected method generates approximate solutions for different values of fractional order μ as shown in Figure 7. Subfigure (a) presents the solution for $\mu = 0.5$, subfigure (b) for $\mu = 0.7$, and

subfigure (c) for $\mu = 1.0$. The solution profiles for $\gamma = 0.1$ show the impact of fractional-order parameter μ for values $0.5, 0.7$, and 1.0 in subfigure (d). The solution profiles show a gradual transformation as μ changes because this fractional-order parameter makes the model more responsive to dynamic properties.

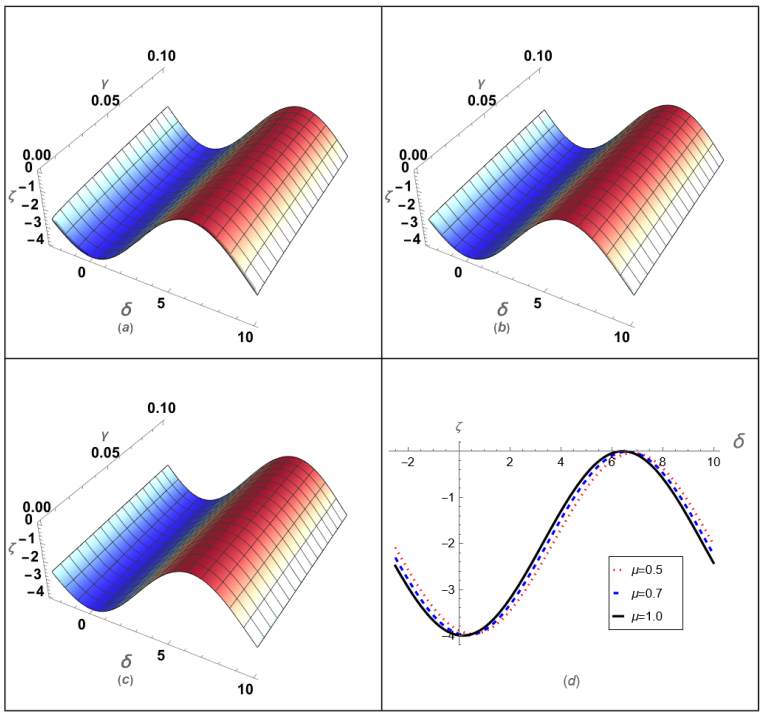

Figure 7. (a) Approximate solution for $\mu = 0.5$; (b) approximate solution for $\mu = 0.7$; (c) approximate solution for $\mu = 1.0$; (d) approximate solution comparison for $\mu = 0.5, 0.7$, and 1.0 at $\gamma = 0.1$.

The approximate response compares with the exact solution in Figure 8 while both solutions have $\mu = 1.0$ for a γ value of 0.1. The matching results between the two solutions proves that the adopted methodology delivers both high accuracy and reliability. The validation process through comparative analysis guarantees that the proposed approximation approach delivers accurate solution estimates with a small departure from actual values.

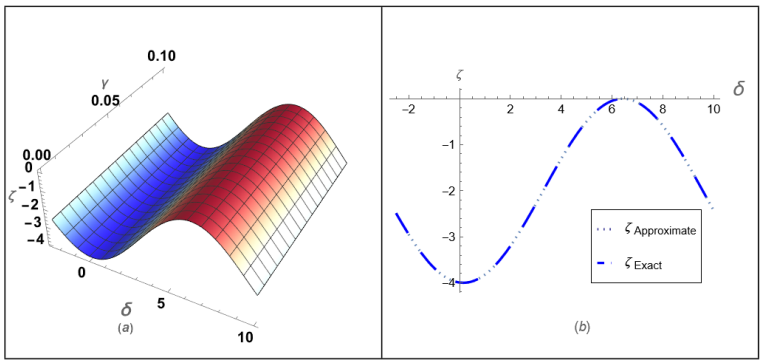

Figure 8. The approximate solution and exact solution comparison for $\mu = 1.0$ and $\gamma = 0.1$.

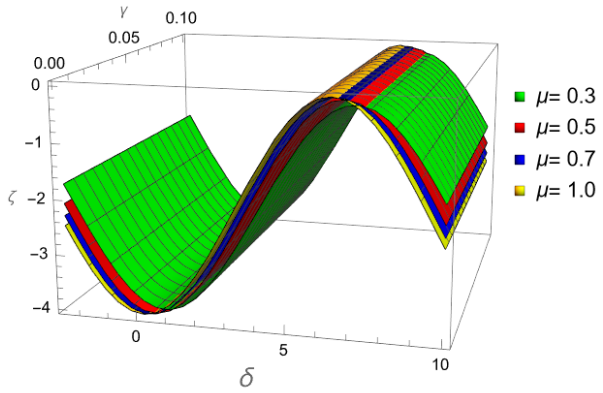

Figure 9. The 3D fractional-order comparison for $\mu = 0.3, 0.5, 0.7$, and 1.0 for $\gamma = 0.1$.

A three-dimensional fractional-order representation shows the results for μ values from 0.3 to 0.7 and 1.0 when γ equals 0.1. The graphical depiction of the solution surface reveals the impact that varying the fractional-order parameter has on the solution. The solution methods must take into account the changing amplitude and wave structures because the varied fractional orders reveal complex patterns in fractional differential equations.

Solution $\zeta(\delta, \gamma)$ shows its response under fractional order $\mu = 1.0$ when γ equals 0.10 based on the data in Table 4. The author conducted four methodological investigations for numerical example 2, namely LRPSM, LLSRPSM, LVIM, and LLSVIM. The provided table enables users to evaluate both the precision and convergence levels of each solution approach. Numerical value consistency between various solution techniques demonstrates the reliable performance of the proposed methods and reveals minor variations that stem from fundamental characteristics of each method. All information about solution behavior across different fractional orders can be found through analysis of the presented figures and tables. Double graphical comparison of numerical solutions with exact solutions helps prove calculation accuracy, and the additional 3D graphs and tables strengthen the research findings. Researchers along with practitioners who study fractional-order nonlinear differential equations in applied mathematics and physics obtain useful information from these analytical findings.

Table 4. The effect of fractional-order $\mu = 1.0$ on the solution $\zeta(\delta, \gamma)$ at $\gamma = 0.10$ obtained through $LRPSM$, $LLSRPSM$, $LVIM$, and $LLSVIM$ for the numerical example 2.

δ	$\zeta(\delta,\gamma)_{LRPSM}$	$\zeta(\delta,\gamma)_{LLSRPSM}$	$\zeta(\delta,\gamma)_{LVIM}$	$\zeta(\delta,\gamma)_{LLSVIM}$	*Exact*	AE of LLSRPSM	AE of LLSVIM
1	-3.82214255	-3.82207319	-3.82214255	-3.82207319	-3.82207746	4.27428752×10^{-6}	4.27428752×10^{-6}
2	-3.20378605	-3.20366720	-3.20378605	-3.20366720	-3.20366918	1.97648334×10^{-6}	1.97648334×10^{-6}
3	-2.29070075	-2.29056151	-2.29070075	-2.29056151	-2.29056070	8.05232887×10^{-7}	8.05232887×10^{-7}
4	-1.30644176	-1.30631622	-1.30644176	-1.30631622	-1.30631283	3.38980002×10^{-6}	3.38980002×10^{-6}
5	-0.49199002	-0.49190891	-0.49199002	-0.49190891	-0.49190377	5.14442589×10^{-6}	5.14442589×10^{-6}
6	-0.04675171	-0.04673490	-0.04675171	-0.04673490	-0.04672926	5.63951689×10^{-6}	5.63951689×10^{-6}
7	-0.07973671	-0.07978831	-0.07973671	-0.07978831	-0.07978355	4.75385746×10^{-6}	4.75385746×10^{-6}
8	-0.58286912	-0.58297650	-0.58286912	-0.58297650	-0.58297380	2.70428793×10^{-6}	2.70428793×10^{-6}
9	-1.43296460	-1.43310147	-1.43296460	-1.43310147	-1.43310148	7.38559968×10^{-9}	7.38559990×10^{-9}
10	-2.42189012	-2.42202297	-2.42189012	-2.42202297	-2.42202568	2.71725088×10^{-6}	2.71725088×10^{-6}

7. Conclusions

In this study, we successfully developed and applied two novel methods, the Laplace least squares residual power series method (LLSRPSM) and the Laplace least squares variational iteration method (LLSVIM), to solve the fractional damped Burgers' equation. By integrating Laplace transforms with least square techniques, we addressed the challenges posed by the nonlinear and fractional nature of the equation. The use of Caputo fractional operators provided a rigorous mathematical foundation for modeling the fractional derivatives, ensuring accurate representation of the system's memory and non-local effects.

The proposed methods demonstrated remarkable efficiency and accuracy in obtaining approximate solutions, as evidenced by numerical results and comparisons with existing techniques. The combination of Laplace transforms and least square minimization not only simplified the solution process but also enhanced the precision of the results. These approaches offer a powerful and versatile framework for solving a wide range of nonlinear fractional differential equations, extending their applicability to various scientific and engineering problems.

Future work could explore the application of these methods to other complex fractional models, as well as further optimization of the computational algorithms to handle higher-dimensional systems. Overall, this study contributes significantly to the field of fractional calculus and provides a promising direction for solving challenging nonlinear fractional differential equations.

Author contributions

M. Mossa Al-Sawalha: Conceptualization, Writing-review & editing; Khalil Hadi Hakami: Visualization, Writing-review & editing, Data curation; Mohammad Alqudah: Data curation, Project administration; Qasem M. Tawhari: Resources, Validation, Software; Hussain Gissy: Formal analysis, Investigation, Resources. All authors have read and agreed to the published version of the manuscript.

Use of Generative-AI tools declaration

The authors declare that they have not used Artificial Intelligence (AI) tools in the creation of this article.

Acknowledgments

The authors gratefully acknowledge the funding of the Deanship of Graduate Studies and Scientific Research, Jazan University, Saudi Arabia, through project number: (RG24-S053)

Conflict of interest

The authors declare that they have no conflicts of interest.

References

1. C. Ionescu, A. Lopes, D. Copot, J. A. T. Machado, J. H. T. Bates, The role of fractional calculus in modeling biological phenomena: A review, *Commun. Nonlinear Sci. Numer. Simul.*, **51** (2017), 141–159. https://doi.org/10.1016/j.cnsns.2017.04.001
2. M. Sinan, K. Shah, P. Kumam, I. Mahariq, K. J. Ansari, Z. Ahmad, et al., Fractional order mathematical modeling of typhoid fever disease, *Results Phys.*, **32** (2022), 105044. https://doi.org/10.1016/j.rinp.2021.105044
3. S. L. Wu, M. Al-Khaleel, Convergence analysis of the Neumann-Neumann waveform relaxation method for time-fractional RC circuits, *Simul. Model. Pract. Theory*, **64** (2016), 43–56. https://doi.org/10.1016/j.simpat.2016.01.002
4. Y. Sun, J. Lu, M. Zhu, A. A. Alsolami, Numerical analysis of fractional nonlinear vibrations of a restrained cantilever beam with an intermediate lumped mass, *J. Low Freq. Noise, Vibrat. Active Control*, **44** (2024), 178–189. https://doi.org/10.1177/14613484241285502
5. S. L. Wu, M. Al-Khaleel, Parameter optimization in waveform relaxation for fractional-order *RC* circuits, *IEEE Trans. Circuits Syst. I: Regular Papers*, **64** (2017), 1781–1790. https://doi.org/10.1109/TCSI.2017.2682119
6. J. Wang, X. Jiang, X. Yang, H. Zhang, A compact difference scheme for mixed-type time-fractional black-Scholes equation in European option pricing, *Math. Meth. Appl. Sci.*, **48** (2025), 6818–6829. https://doi.org/10.1002/mma.10717
7. T. Liu, H. Zhang, X. Yang, The ADI compact difference scheme for three-dimensional integro-partial differential equation with three weakly singular kernels, *J. Appl. Math. Comput.*, 2025. https://doi.org/10.1007/s12190-025-02386-3
8. K. Liu, Z. He, H. Zhang, X. Yang, A Crank-Nicolson ADI compact difference scheme for the three-dimensional nonlocal evolution problem with a weakly singular kernel, *Comp. Appl. Math.*, **44** (2025), 164. https://doi.org/10.1007/s40314-025-03125-x
9. Z. Chen, H. Zhang, H. Chen, ADI compact difference scheme for the two-dimensional integro-differential equation with two fractional Riemann-Liouville integral kernels, *Fractal Fract.*, **8** (2024), 707. https://doi.org/10.3390/fractalfract8120707
10. X. Yang, W. Wang, Z. Zhou, H. Zhang, An efficient compact difference method for the fourth-order nonlocal subdiffusion problem, *Taiwanese J. Math.*, **29** (2025), 35–66. https://doi.org/10.11650/tjm/240906
11. D. Baleanu, Z. B. Guvenc, J. T. Machado, *New trends in nanotechnology and fractional calculus applications*, New York: Springer, 2010.
12. N. H. Sweilam, M. M. Abou Hasan, D. Baleanu, New studies for general fractional financial models of awareness and trial advertising decisions, *Chaos Solit. Fract.*, **104** (2017), 772–784. https://doi.org/10.1016/j.chaos.2017.09.013
13. D. Baleanu, G. C. Wu, S. D. Zeng, Chaos analysis and asymptotic stability of generalized Caputo fractional differential equations, *Chaos Solit. Fract.*, **102** (2017), 99–105. https://doi.org/10.1016/j.chaos.2017.02.007

14. P. Veeresha, D. G. Prakasha, H. Mehmet Baskonus, New numerical surfaces to the mathematical model of cancer chemotherapy effect in Caputo fractional derivatives, *Chaos: Interdiscipl. J. Nonlinear Sci.*, **29** (2019), 013119. https://doi.org/10.1063/1.5074099

15. S. Noor, H. A. Alyousef, A. Shafee, R. Shah, S. A. El-Tantawy, A novel analytical technique for analyzing the (3+ 1)-dimensional fractional calogero-bogoyavlenskii-schiff equation: investigating solitary/shock waves and many others physical phenomena, *Phys, Scr.*, **99** (2024), 065257. https://doi.org/10.1088/1402-4896/ad49d9

16. E. F. D. Goufo, Application of the Caputo-Fabrizio fractional derivative without singular kernel to Korteweg-de Vries-Burgers's equation, *Math. Model. Anal.*, **21** (2016), 188–198. https://doi.org/10.3846/13926292.2016.1145607

17. A. A. Kilbas, H. M. Srivastava, J. J. Trujillo, *Theory and applications of fractional differential equations*, Amsterdam: Elsevier, 2006.

18. X. Yang, Z. Zhang, Superconvergence analysis of a robust orthogonal Gauss collocation method for 2D fourth-order subdiffusion equations, *J. Sci. Comput.*, **100** (2024), 62. https://doi.org/10.1007/s10915-024-02616-z

19. X. Shen, X. Yang, H. Zhang, The high-order ADI difference method and extrapolation method for solving the two-dimensional nonlinear parabolic evolution equations, *Mathematics*, **12** (2024), 3469. https://doi.org/10.3390/math12223469

20. Y. Shi, X. Yang, Z. Zhang, Construction of a new time-space two-grid method and its solution for the generalized Burgers' equation, *Appl. Math. Lett.*, **158** (2024), 109244. https://doi.org/10.1016/j.aml.2024.109244

21. X. Yang, Z. Zhang, Analysis of a new NFV scheme preserving DMP for two-dimensional sub-diffusion equation on distorted meshes, *J. Sci. Comput.*, **99** (2024), 80. https://doi.org/10.1007/s10915-024-02511-7

22. X. Yang, Z. Zhang, On conservative, positivity preserving, nonlinear FV scheme on distorted meshes for the multi-term nonlocal Nagumo-type equations, *Appl. Math. Lett.*, **150** (2024), 108972. https://doi.org/10.1016/j.aml.2023.108972

23. Q. Wang, Homotopy perturbation method for fractional KdV-Burgers's equation, *Chaos Solit. Fract.*, **35** (2008), 843850. https://doi.org/10.1016/j.chaos.2006.05.074

24. S. Anil Sezer, A. Yildırım, S. Tauseef Mohyud-Din, He's homotopy perturbation method for solving the fractional KdV-Burgers's-Kuramoto equation, *Int. J. Numer. Meth. Heat Fluid Flow*, **21** (2011), 448–458.

25. G. C. Wu, D. Baleanu, Variational iteration method for the Burgers's' flow with fractional derivatives-new Lagrange multipliers, *Appl. Math. Model.*, **37** (2013), 6183–6190. https://doi.org/10.1016/j.apm.2012.12.018

26. M. Inc, The approximate and exact solutions of the space-and time-fractional Burgers's equations with initial conditions by variational iteration method, *J. Math. Anal. Appl.*, **345** (2008), 476–484. https://doi.org/10.1016/j.jmaa.2008.04.007

27. A. Esen, N. M. Yagmurlu, O. Tasbozan, Approximate analytical solution to time-fractional damped Burgers' and Cahn-Allen equations, *Appl. Math. Inf. Sci.*, **7** (2013), 1951–1956. http://doi.org/10.12785/amis/070533

28. H. Jafari, V. Daftardar-Gejji, Solving linear and nonlinear fractional diffusion and wave equations by Adomian decomposition, *Appl. Math. Comput.*, **180** (2006), 488–497. https://doi.org/10.1016/j.amc.2005.12.031

29. J. Lu, Y. Sun, Numerical approaches to time fractional boussinesq-burgers equations, *Fractals*, **29** (2021), 2150244. https://doi.org/10.1142/S0218348X21502443

30. J. Singh, D. Kumar, M. A. Qurashi, Baleanu, Analysis of a new fractional model for damped Bergers' equation, *Open Phys.*, **15** (2017), 35–41. https://doi.org/10.1515/phys-2017-0005

31. B. M. Vaganan, M. S. Kumaran, Kummer function solutions of damped Burgers's equations with time-dependent viscosity by exact linearization, *Nonlinear Anal.: Real World Appl.*, **9** (2008), 2222–2233. https://doi.org/10.1016/j.nonrwa.2007.08.001

32. W. Malfliet, Approximate solution of the damped Burgers's equation, *J. Phys. A: Math. Gen.*, **26** (1993), L723. https://doi.org/10.1088/0305-4470/26/16/003

33. F. Yilmaz, B. Karasozen, Solving optimal control problems for the unsteady Burgers's equation in COMSOL Multiphysics, *J. Comput. Appl. Math.*, **235** (2011), 4839–4850. https://doi.org/10.1016/j.cam.2011.01.002

34. P. Rosenau, J. M. Hyman, Compactons: solitons with finite wavelength, *Phys. Rev. Lett.*, **70** (1993), 564. https://doi.org/10.1103/PhysRevLett.70.564

35. B. Mihaila, A. Cardenas, F. Cooper, A. Saxena, Stability and dynamical properties of Rosenau-Hyman compactons using Pade approximants, *Phys. Rev. E-Stat. Nonlinear Soft Matter Phys.*, **81** (2010), 056708. https://doi.org/10.1103/PhysRevE.81.056708

36. F. Rus, F. R. Villatoro, Self-similar radiation from numerical Rosenau-Hyman compactons, *J. Comput. Phys.*, **227** (2007), 440–454. https://doi.org/10.1016/j.jcp.2007.07.024

37. F. Rus, F. R. Villatoro, Numerical methods based on modified equations for nonlinear evolution equations with compactons, *Appl. Math. Comput.*, **204** (2008), 416–422. https://doi.org/10.1016/j.amc.2008.06.056

38. O. S. Iyiola, G. O. Ojo, O. Mmaduabuchi, The fractional Rosenau-Hyman model and its approximate solution, *Alex. Eng. J.*, **55** (2016), 1655–1659. https://doi.org/10.1016/j.aej.2016.02.014

39. J. Singh, D. Kumar, R. Swroop, S. Kumar, An efficient computational approach for time-fractional Rosenau-Hyman equation, *Neural Comput. Applic.*, **30** (2018), 3063–3070. https://doi.org/10.1007/s00521-017-2909-8

40. R. Yulita Molliq, M. S. M. Noorani, Solving the fractional Rosenau-Hyman equation via variational iteration method and homotopy perturbation method, *Int. J. Differ. Equ.*, **2012** (2012), 472030. https://doi.org/10.1155/2012/472030

41. M. Senol, O. Tasbozan, A. Kurt, Comparison of two reliable methods to solve fractional Rosenau-Hyman equation, *Math. Meth. Appl. Sci.*, **44** (2021), 7904–7914. https://doi.org/10.1002/mma.5497

42. M. Cinar, A. Secer, M. Bayram, An application of Genocchi wavelets for solving the fractional Rosenau-Hyman equation, *Alex. Eng. J.*, **60** (2021), 5331–5340. https://doi.org/10.1016/j.aej.2021.04.037

43. S. O. Ajibola, A. S. Oke, W. N. Mutuku, LHAM approach to fractional order Rosenau-Hyman and Burgers' equations, *Asian Res. J. Math.*, **16** (2020), 1–14. https://doi.org/10.9734/ARJOM/2020/v16i630192

44. M. Alaroud, Application of Laplace residual power series method for approximate solutions of fractional IVP's, *Alex. Eng. J.*, **61** (2022), 1585–1595. https://doi.org/10.1016/j.aej.2021.06.065

45. M. Alquran, M. Ali, M. Alsukhour, I. Jaradat, Promoted residual power series technique with Laplace transform to solve some time-fractional problems arising in physics, *Results Phys.*, **19** (2020), 103667. https://doi.org/10.1016/j.rinp.2020.103667

46. H. Aljarrah, M. Alaroud, A. Ishak, M. Darus, Approximate solution of nonlinear time-fractional PDEs by Laplace residual power series method, *Mathematics*, **10** (2022), 1980. https://doi.org/10.3390/math10121980

47. A. Shafee, Y. Alkhezi, R. Shah, Efficient solution of fractional system partial differential equations using Laplace residual power series method, *Fractal Fract.*, **7** (2023), 429. https://doi.org/10.3390/fractalfract7060429

48. M. N. Oqielat, T. Eriqat, O. Ogilat, A. El-Ajou, S. E. Alhazmi, S. Al-Omari, Laplace-residual power series method for solving time-fractional reaction-diffusion model, *Fractal Fract.*, **7** (2023), 309. https://doi.org/10.3390/fractalfract7040309

49. N. Anjum, J. H. He, Laplace transform: making the variational iteration method easier, *Appl. Math. Lett.*, **92** (2019), 134–138. https://doi.org/10.1016/j.aml.2019.01.016

50. N. Bildik, A. Konuralp, The use of variational iteration method, differential transform method and Adomian decomposition method for solving different types of nonlinear partial differential equations, *Int. J. Nonlinear Sci. Numer. Simul.*, **7** (2006), 65–70. https://doi.org/10.1515/IJNSNS.2006.7.1.65

51. N. A. Shah, I. Dassios, E. R. El-Zahar, J. D. Chung, S. Taherifar, The variational iteration transform method for solving the time-fractional Fornberg-Whitham equation and comparison with decomposition transform method, *Mathematics*, **9** (2021), 141. https://doi.org/10.3390/math9020141

52. S. M. Kenneth, B. Ross, *An introduction to the fractional calculus and fractional differential equations*, Hoboken: Wiley, 1993.

53. R. Almeida, D. F. Torres, Calculus of variations with fractional derivatives and fractional integrals, *Appl. Math. Lett.*, **22** (2009), 1816–1820. https://doi.org/10.1016/j.aml.2009.07.002

54. R. Almeida, D. F. Torres, Necessary and sufficient conditions for the fractional calculus of variations with Caputo derivatives, *Commun. Nonlinear Sci. Numer. Simul.*, **16** (2011), 1490–1500. https://doi.org/10.1016/j.cnsns.2010.07.016

55. O. Agrawal, Fractional variational calculus in terms of Riesz fractional derivatives, *J. Phys. A: Math. Theor.*, **40** (2007), 6287. https://doi.org/10.1088/1751-8113/40/24/003

56. R. Kumar, R. Koundal, Generalized least square homotopy perturbations for system of fractional partial differential equations, preprint paper, 2018. https://doi.org/10.48550/arXiv.1805.06650

57. A. El-Ajou, Adapting the Laplace transform to create solitary solutions for the nonlinear time-fractional dispersive PDEs via a new approach, *Eur. Phys. J. Plus*, **136** (2021), 229. https://doi.org/10.1140/epjp/s13360-020-01061-9

58. Z. Korpinar, M. Inc, E. Hınçal, D. Baleanu, Residual power series algorithm for fractional cancer tumor models, *Alex. Eng. J.*, **59** (2020), 1405–1412. https://doi.org/10.1016/j.aej.2020.03.044

59. J. Zhang, Z. Wei, L. Li, C. Zhou, Least-squares residual power series method for the time-fractional differential equations, *Complexity*, **2019** (2019), 6159024. https://doi.org/10.1155/2019/6159024

AIMS Press